LOCATING THE IRIS: A FIRST STEP TO REGISTRATION AND IDENTIFICATION

N. Ritter
Murdoch University
Australia

J. R. Cooper
Curtin University of Technology
Australia

ABSTRACT
This paper presents a method for locating the iris borders in images of the cornea. It uses a combination of *a priori* information, statistics and active contours to both find the iris borders and assess its own success or failure. When applied to 107 images from 11 different people with varying eye colours including light blue and dark brown the algorithm reports 7 images for which it failed to find the borders, one of which was a false negative. In the other 100 images, the algorithm located the iris borders with average estimated errors of 5.0 pixels for the left iris-sclera border, 3.4 pixels for the right iris-sclera border and 2.1 pixels for the pupil-iris border. There were no false positive results.

KEY WORDS
Circular Active Contour, Iris, Registration, Identification

1 Introduction

The cornea is the 0.5mm thick transparent layer that allows light to enter the eye whilst protecting the internal components of the eye from dust and other intrusions. Registration of images of the cornea has applications in the fields of biometric identification and ophthalmology. In the former of these it is necessary to register images in order to compare iris striations to ascertain if the two images belong to the same person. In ophthalmology registration allows identification of changes in images taken at different times, and—with the addition of a slit of light—assists in diagnosis of medical problems [1]. Multiple slit-lamp images can also be used to provide topographic information of the cornea [2].

Registration of corneal images is complicated by movement of the head, eye, iris and eyelids; occlusion of the eye by the eyelids or eyelashes; specular reflections on the cornea and iris; and different eye colours—and hence image grey levels—of eye images. Standard whole image registration techniques generally rely on searching for a minimum of a specific similarity value. These methods have not proved to be robust for corneal images because the feature density of the eyelashes cause the images to align these, rather than the eye itself. Template matching techniques require the selection of a template in the reference image, which requires prior knowledge of the location of a feature within the part of the image that shows the cornea.

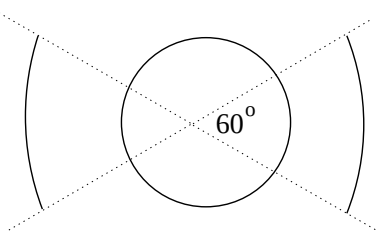

Figure 1. The model of the eye used for locating the pupil-iris and iris-sclera borders. The inner border is a DCAC, the outer border is a DCAC with most of the nodes 'switched off' so that they do not affect the movement of the contour

It therefore seems useful to commence by locating the iris in corneal images, prior to processing them for identification or registration. This paper describes a new method of locating the iris within an image of the cornea, using the *a priori* information that the iris in such images can be modeled as a non-concentric partial annulus, as shown in Fig. 1.

2 Literature Review

There has been relatively little research on registration of corneal images or location of the pupil or iris within such images. Eye tracking research is clearly related, but generally relies on image thresholding to produce an image in which the pupil forms the largest dark mass [3]. However when attempting to apply this method to images taken with a slit-lamp bio-microscope—standard ophthalmological equipment—there proved to be no threshold that would work for all eye colours, even when pre-processed in a variety of ways. Eye-torsion research [4, 5] also studies corneal images, however again the assumption is that the pupil will be found at the centroid of a thresholded binary image.

Daugman [6] develops a method in which the pupil-iris border is found by searching over all circles for the circle That gives the most abrupt and sudden change in pixel intensity. Once the pupil-iris border has been found, the iris-sclera border is found with a similar method that

uses horizontally exploding pie-wedges to deal with the problems of eyelid occlusion and circular iris features. However this algorithm has been patented by Daugman and is therefore unavailable.

3 Locating the Pupil-Iris and Iris-Sclera Borders

3.1 Discrete Circular Active Contours

Active contours have already proved to be useful in location of features within images [7]. Since the pupil-iris border is circular it is useful to define an active contour that, given a starting point, locates a circle within an image.

We propose a Discrete Circular Active Contour (DCAC) composed of n vertices connected as a simple closed curve with internal and external forces acting on the vertices [8]. The internal force applied to each vertex pushes it outwards attempting to force the contour into a perfect polygon with a radius δ larger than the current average radius, thus applying the *a priori* information of circularity *globally* rather than locally as do Gunn & Nixon [9]. The application of global circularity reduces local deformations produced by specular reflections and dark patches of iris near the pupil-iris border. Fig. 2 shows the application of this model diagrammatically. The internal force, $\mathbf{F}_{int,i}$, for each vertex, v_i, can therefore be defined mathematically by

$$\mathbf{F}_{int,i} = \tilde{v}_i - v_i, \tag{1}$$

where $\tilde{v}_i$ is the position of this vertex in the perfect polygon. If C_r is the average radius of the current contour and $C = (C_x, C_y)$ is the current centroid, then

$$\tilde{v}_i = \left(C_x + (C_r + \delta)\cos\left(\frac{2\pi i}{n}\right) , \right.$$
$$\left. C_y + (C_r + \delta)\sin\left(\frac{2\pi i}{n}\right)\right), \tag{2}$$

where n is the number of nodes; δ is the increase in the radius at each iteration; the centroid C is defined by

$$C = \frac{1}{n}\sum_{i=1}^{n} v_i \; ; \tag{3}$$

and the average radius C_r is defined with

$$C_r = \frac{1}{n}\sum_{i=1}^{n} \|v_i - C\| \; . \tag{4}$$

The image force provided by the grey levels of the pixels in the image must push the vertices inwards to balance the contour's internal force. The direction of this external image force for each vertex v_i is therefore defined as a unit vector given by

$$\hat{\mathbf{F}}_{im,i} = \frac{C - v_i}{\|C - v_i\|}, \tag{5}$$

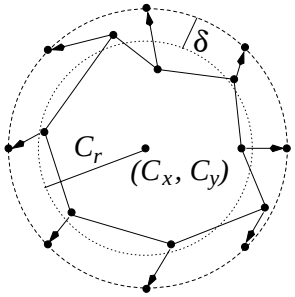

Figure 2. The internal force on each vertex pushes it towards the matching vertex of a perfect polygon of radius δ more than the current average radius

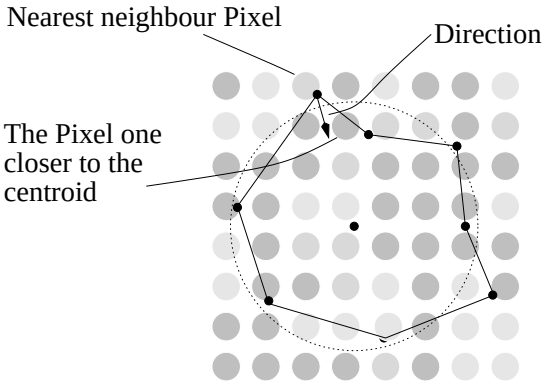

Figure 3. The image force on each vertex pushes it towards the contour's centroid with a magnitude given by the difference between grey level values of its nearest neighbour and the nearest pixel one closer to the centroid

and its magnitude is defined with

$$\|\mathbf{F}_{im,i}\| = I(v_i) - I(v_i + \hat{\mathbf{F}}_{im,i}), \quad (6)$$

where $I(v_i)$ is the grey level value of the nearest neighbour to v_i. Therefore the image force for each vertex is given by

$$\mathbf{F}_{im,i} \quad = \quad \|\mathbf{F}_{im,i}\| \, \hat{\mathbf{F}}_{im,i}. \quad (7)$$

A schematic diagram showing an image force can be seen in Fig. 3.

The movement of the contour is defined as the sum of the internal and image forces, therefore the vertex moves from iteration t to $t+1$ using

$$v_i(t+1) = v_i(t) + \beta \mathbf{F}_{int,i} + (1-\beta)\mathbf{F}_{im,i}, \quad (8)$$

where β weights the two forces. This movement then continues until either equilibrium occurs or an error condition occurs. Equilibrium is considered to have been reached when the average radius and centre of the current contour is the same as the contour found m iterations ago. This ensures that even if individual vertices are moving—they sometimes oscillate—the contour itself can be deemed to be stationary.

3.2 Using a DCAC to Find an Iris Border

The algorithm given in Section 3.1 could in principle find either the pupil-iris border or the iris-sclera border depending on the starting configuration, because in each case the border is circular with the inside region being darker. Unfortunately, several problems occur with such a simple approach when used with images of real eyes.

Firstly, the DCAC search for the pupil-iris border is frequenly affected by specular reflections from the cornea. This problem can be resolved by performing the inner DCAC movement on pre-processed images where all pixels brighter than 128 have been set to 128.

The second problem is that in images of real eyes the algorithm is overly dependent on the value of δ in (2). If δ is too large the contour will always move off the image, if δ is too small the contour will either remain where it starts, grow too slowly for practical purposes, or contract to a radius of zero. Unfortunately there is no value for δ that will work with a wide range of eye images. The optimal value depends on the contrast across the border that is the subject of the search. To solve this problem, a suitable value for δ is found by wrapping the DCAC algorithm in a loop that adjusts the value of δ if that algorithm produces any of these error conditions.

This search for a suitable value of δ leads to its own problems: δ can now grow or shrink or oscillate indefinitely. Therefore, further conditions are introduced ensuring that (a) δ always lies within δ_{min} and δ_{max} (b) the amount by which δ is changed, δ_ϵ, can be reduced to stop oscillation between values of δ and (c) δ_ϵ never becomes less than a minimum value $\delta_{\epsilon min}$.

A further refinement can be made to the algorithm using *a priori* knowledge about the maximum and minimum possible size of the border for which the algorithm is searching. Thus, the algorithm for finding these borders is given by:

Algorithm 1 *Find Iris Border*

```
Initialise δ, δ_ε, δ_ε0, δ_last1 and δ_last2
Initialise bounceError to false
WHILE δ lies between δ_min and δ_max
      AND bouncError is false
      AND the contour is not in equilibrium
    Initialise the contour
    WHILE the contour is not in equilibrium
          AND the contour is in the image
          AND the contour is not too large
          AND the contour is not too small
          AND not maxIterations
        Move the contour points using (8)
    ENDWHILE
    IF the contour is too large
       OR the contour is off the image
        Reduce δ by δ_ε
    ELSE IF the contour is too small
            OR maxIterations was reached
        Increase δ by δ_ε
    ENDIF
    IF equilibrium was not reached
        δ_last2 = δ_last1
        δ_last1 = δ
        IF δ_last2 == δ  [we have oscillation]
            δ_ε = δ_ε / 10  [try a smaller change in δ]
        ENDIF
        IF δ_ε < δ_εmin  [the oscillation cannot be stopped]
            bounceError = true
        ENDIF
    ENDIF
ENDWHILE
```

After this algorithm terminates, either the contour has found equilibrium or the algorithm reports failure because δ has become too large, δ has become too small or δ_ϵ has become too small.

3.3 Finding a Starting Position

Before we can use Algorithm 1 we need to find a starting position for the contour. Whilst it is not possible to find

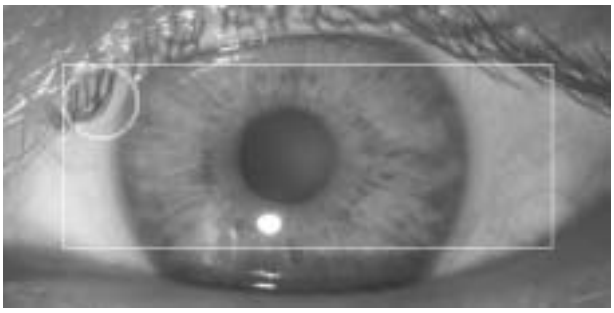

Figure 4. An annular template is used to search the centre portion of an image to find the approximate position of the pupil

a threshold that allows reliable segmentation of the pupil from the rest of the image, it is still true that the pupil forms a circular dark mass within the image. Therefore the first step in our algorithm is to find a circular area of the image that has a low average grey level.

The size and shape of the template to be used for such a search was developed empirically using 9 images from 9 eyes of five people. The eye colours varied from light blue to dark brown. The template that proved optimal in terms of accuracy and speed was an annulus with inner radius 30 pixels and outer radius 32 pixels, as shown in Fig. 4. To improve the time taken, only the centre region of the image is searched, the assumption being that a trained clinical photographer is unlikely to take photographs where the pupil is close to the edge of the image. The centre of the annulus with the lowest average grey level is used to initialise the next phase of the registration method.

3.4 Finding Both Iris Borders

The iris has an annular shape. However part of the outer circle of this annulus is usually obscured by the eyelids. When searching for the iris-sclera border with Algorithm 1 we prevent the algorithm from trying to find obscured parts of the iris-sclera border by using a DCAC with most of its nodes 'switched off' so that they do not affect the movement of the contour. This is illustrated in Fig. 1, which shows the DCAC for the pupil-iris border as a full circle, while the DCAC for the iris-sclera has only two active arcs.

The inner DCAC is seeded with the pupil location found as described in Section 3.3 and allowed to expand outward until it either finds the pupil or fails. If it does not fail, then the information from the position thus reached is used to seed the starting position of the outer DCAC. The centre of the final outer DCAC is then used to seed a second pass of the double DCAC algorithm, improving the success rate significantly.

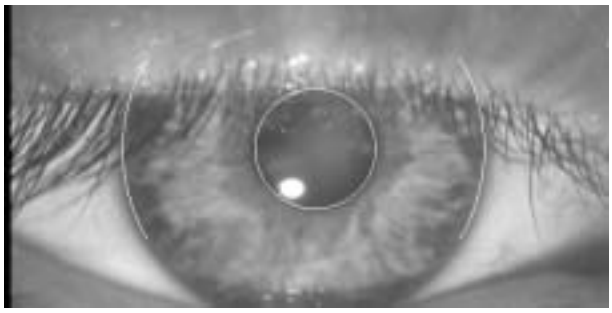

Figure 5. Images such as this one—with the computed average contours drawn in position—were used to analyse the results of the algorithm. This image shows a case where the pupil-iris and iris-sclera borders are found accurately. Note that dark shadows surrounding the iris can only be identified as belonging to the sclera when viewed in high resolution images on screen

Finally, it is useful for the entire algorithm to be able to judge its own success. After the contours have been found, a contour that is correctly running along the iris-sclera border should have different average grey levels on the inside and outside of this border. If these are not different, the algorithm execution can be automatically registered as a fail. Thus, the algorithm produces either an estimate of the iris position or reports a failed search.

4 Results

Sixteen training images taken from six different people with a variety of eye colours were used to empirically find values for the various constants of (1) to (8) and Algorithm 1. The algorithm was then applied to 107 images from 11 different people with varying eye colours including light blue and dark brown. None of these people were in the original training set.

The results were analysed by viewing each image with the computed partial annulus drawn in position as illustrated in Fig. 5. For all images the contours were either close to the true borders or did not match at all.

The algorithm reports failure in 7 (6.5%) of the 107 test images, one of which is a false negative. Table 1 shows these results. Five of the failures occur because the seed point for the contours is not found correctly due to particularly dark patches of the iris or eyelashes. An example of such an image is given in Fig. 6. The sixth failure occurs because the iris is not fully on the images—which is the correct response for the algorithm—and the false negative is confused by a circular iris striation.

To analyse the accuracy of the 93.5% of images for which the borders were found, the point of worst

Table 1. The results of the self-assessment when applying the algorithm to 107 images from 11 different people with varying eye colours including light blue and dark brown. There was only one false-negative and no false-positives.

Algorithm Report	Iris Found	No. of Images	% of Images
Fail	No	6	5.6
Fail	Yes	1	0.9
Success	No	0	0.0
Success	Yes	100	93.5

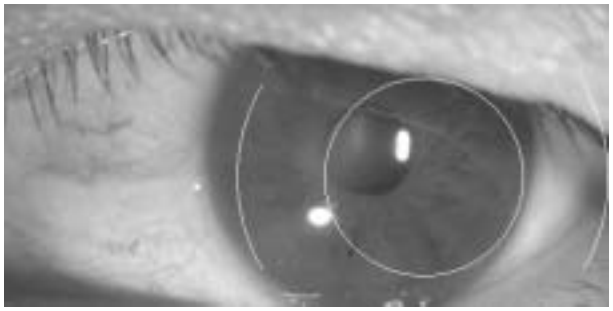

Figure 6. An image for which the contour algorithm failed to find the contour. Note that this failure is reported by the algorithm itself.

agreement was located by sight for the pupil-iris and iris-sclera borders. The distance between the perceived and calculated border positions at this point is then reported as a measure of estimated error.

In each such case, the iris-sclera error is 17 pixels or less and the pupil-iris error is 6 pixels or less. An error of 17 pixels is small enough for a subsequent refinement process. Furthermore, as can be seen in the example in Fig. 7, an error this large only appears on one side of the iris in any image.

The average error in the left iris-sclera border is 5.0 pixels, in the right iris-sclera border it is 3.4 pixels and for the pupil-iris border it is 2.1 pixels. A summary of these results can be seen in Table 4, and graphs of the distribution of these estimated errors can be seen in Fig. 8. An example of estimated high accuracy can be seen in Fig. 5 and an example of estimated poor accuracy in Fig. 7. There is no eye for which the algorithm fails for all images, and there are no false positives.

5 Conclusion

We present an algorithm that combines the use of statistics with a new discrete circular active contour. The algorithm

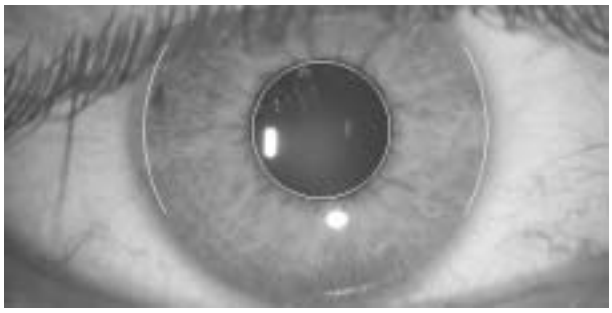

Figure 7. An example where the output result had an estimated error of 16 pixels. This result is close enough to act as a seed for a subsequent refinement process

Table 2. The manually estimated errors for the 100 images for which the contour algorithm reports success.

Border	Min Error	Max Error	Mean Error	Std. Dev. Error
left iris-sclera	0	17	5.0	2.7
right iris-sclera	0	9	3.4	1.9
pupil-iris	0	6	2.1	1.4

is successful enough to provide a good starting point for a subsequent refinement of iris position and self-assesses its result to reject images where the search has failed. Once the iris position has been refined it may be used for either registration or identification.

Acknowledgments

The authors would like to thank The Lions Eye Institute, Perth for financial support of the early parts of this research. They would also like to thank Chris Barry of that institute for taking the photographs.

References

[1] C. L. Martonyi, C. F. Bahn, and R. F. Meyer, *Clinical Slit Lamp Biomicroscopy and Photo Slit Lamp Biomicrography*. (Michigan: Time One Ink, Ltd., 1985).

[2] V. Yaylali, S. C. Kaufman, and H. W. Thompson, Corneal thickness measurements with the orbscan topography system and ultrasonic pachymetry, *Journal of Cataract & Refractive Surgery*, 23(9), 1997, 1345–50.

[3] A. H. Clarke, W. Teiwes, and H. Scherer, Video-oculography - an alternative method for measurement of three-dimensional eye movements, in R. Schmid and

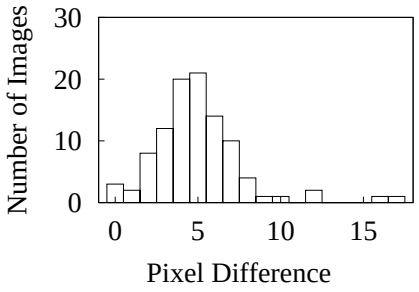

(a) A histogram of the estimated errors for the left iris-sclera border

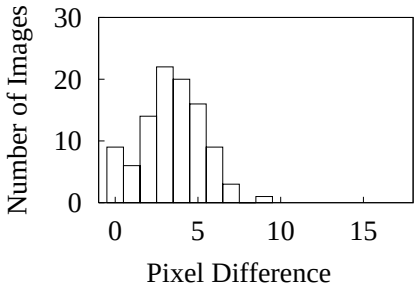

(b) A histogram of the estimated errors for the right iris-sclera border

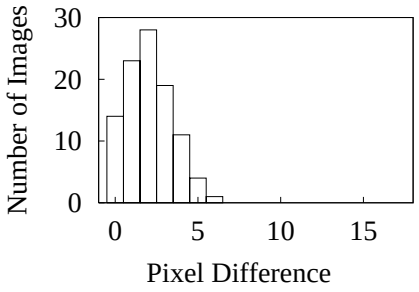

(c) A histogram of the estimated errors for the pupil-iris border

Figure 8. These histograms show the spread of estimated errors for those images for which the algorithm reports successfully finding the iris borders

D. Zambarbieri (Eds), *Oculomotor Control and Cognitive Processes*, (New York: Elsevier Science Publishers, 1991) 431–443.

[4] S. T. Moore, T. Haslwanter, I. S. Curthoys, and S. T. Smith, A geometric basis for measurement of three-dimensional eye position using image processing, *Vision Research*, 36(3), 1996, 445–459.

[5] E. Groen, J. E. Bos, P. F. M. Nacken, and B. de Graaf, Determination of ocular torsion by means of automatic pattern recognition, *IEEE Transactions on Biomedical Engineering*, 43(5), 1996, 471–479.

[6] J. G. Daugman, *Biometric personal identification system based on iris analysis*, (Canberra: Patent Office, 1994).

[7] A. K. Jain, Y. Zhong, and M.-P. Dubuisson-Jolly, Deformable template models: a review, *Signal Processing*, 71(2), 1998, 109–129.

[8] S. Lobregt and M. A. Viergever, A discrete dynamic contour model, *IEEE Transactions on Medical Imaging*, 14(1), 1995, 12–24.

[9] S. R. Gunn and M. S. Nixon, Robust snake implementation - a dual active contour, *IEEE Transactions on Pattern Analysis and Machine Intelligence*, 19(1), 1997, 63–68.